Mycological Progress (2022) 21:81
https://doi.org/10.1007/s11557-022-01832-x

ORIGINAL ARTICLE

Studies in *Gyromitra* II: cryptic speciation in the *Gyromitra gigas* species complex; rediscovery of *G. ussuriensis* and *G. americanigigas* sp. nov.

Andrew N. Miller[1] · Alden C. Dirks[2] · Nina Filippova[3] · Eugene Popov[4] · Andrew S. Methven[5]

Received: 2 June 2022 / Revised: 3 August 2022 / Accepted: 5 August 2022

Abstract

Taxa in the *Gyromitra gigas* species complex were previously studied and their taxonomy resolved. During ongoing studies in this group, cryptic speciation was discovered in *G. gigas*. Sequences of the ITS and LSU regions from 75 specimens were included in maximum likelihood and Bayesian phylogenetic analyses to establish species boundaries and resolve species relationships. Sequence similarity comparisons were also conducted between the two ribosomal markers and between the ITS1 and ITS2 regions. *Gyromitra gigas sensu stricto* and two additional species were discovered within the *G. gigas* clade. *Gyromitra ussuriensis* was rediscovered as a distinct taxon and removed from synonymy under *G. gigas*. It occurs in central and eastern Asia, whereas *G. gigas* occurs mostly in Europe but also extends into central Asia. A neotype is designated for *G. ussuriensis*. A new species, *Gyromitra americanigigas*, is described and illustrated from eastern North America. Although morphology and the LSU exhibited little variation among the three species, the ITS1 and ITS2 regions displayed similar interspecific sequence variability around 0.5–1%, which is sufficient for species identification at the molecular level.

Keywords *Ascomycota* · Fungi · ITS sequences · *Pezizales* · Molecular systematics · 1 new taxon · 1 new typification

Introduction

The *Gyromitra gigas* species complex consists of six taxa: *G. gigas* (Krombh.) Quél., *G. khanspurensis* Jabeen & Khalid, *G. korfii* (Raitv.) Harmaja, *G. montana* Harmaja, *G. pseudogigas* X.C. Wang & W.Y. Zhuang, and *G. ticiniana* Littini. Type specimens have been designated and sequenced, taxonomy and associated nomenclature have been reconciled, and species concepts and biogeographical distributions have been resolved through molecular and morphological analyses for all six species in this complex (Krisai-Greilhuber et al. 2017; Carbone et al. 2018; Wang and Zhuang 2019; Miller et al. 2020).

Gyromitra gigas is a widespread taxon that is infrequently collected throughout Europe (Carbone et al. 2018), but has also been reported from China, Japan, North America, and Russia (MyCoPortal 2022). An epitype (MBT 383600) specimen has been designated from the Czech Republic (Carbone et al. 2018). It is reported to grow near or on rotten logs and old stumps in woods of *Abies*, *Betula*, *Carpinus*, *Picea*, *Populus tremula*, *Quercus*, and *Tilia* from mid-March to early May (Carbone et al. 2018). ITS sequence data has recently shown its distribution to be limited to Europe, with single reports from China and Russia (Miller et al. 2020). Although the European name *G. gigas* has been frequently used for North American material, this species does not occur in North America. Rather, *G. korfii* occurs throughout eastern North America, whereas *G. montana* occurs primarily in western North America and Canada (Miller et al. 2020).

Gyromitra ussuriensis was described in 1950 from the Ussurisky Nature Reserve (formerly known as the Suputinsky Nature Reserve) in Far East Russia (Vassiljeva 1950). It is infrequently collected and reported to grow on

Section Editor: Roland Kirschner

✉ Andrew N. Miller
amiller7@illinois.edu

[1] Illinois Natural History Survey, University of Illinois Urbana-Champaign, Champaign, IL, USA

[2] University of Michigan, Ann Arbor, MI, USA

[3] Yugra State University, Khanty-Mansiysk, Russia

[4] Komarov Botanical Institute, Saint Petersburg, Russia

[5] Leland, NC, USA

Published online: 24 August 2022

rotten logs and stumps of *Pinus koraiensis* and on dead trunks and stumps of *Betula costata* from late May to early June. It was compared to *G. gigas* because of its similar ascospores, but distinguished by the smaller hymenophore with a free edge, longer stem, and its growth on wood (Vassiljeva 1950). Since he found no morphological differences, Raitviir treated *G. ussuriensis* as a synonym of *G. gigas* (Raitviir 1970) where it remains today (Carbone et al. 2018, Index Fungorum).

During our ongoing taxonomic and systematic studies of *Gyromitra* Fr., two well-supported clades occurring near *G. gigas* were discovered that represent cryptic species, one previously described representing *G. ussuriensis* and the other an undescribed species. The goals of this study were to sample and sequence multiple representatives for these two taxa as well as *G. gigas* and to establish species boundaries, reconcile species relationships and biogeographical distributions, and assess the potential of ITS and LSU for resolving these cryptic species.

Materials and methods

Specimens examined

Entire dried ascomata or small portions of the hymenophore of ascomata in 1.5 mL centrifuge tubes were sent to the first author either as loans or as gifts. Sequences generated during this study were obtained from DNA extracted directly from these dried ascomata, which were deposited at ILLS or are available at their home institution (BPI, CUP, F, ILLS, LE, MICH, MIN, NY, O, TAAM, TNS, and YSU). Fungarium acronyms follow Index Herbariorum (Thiers 2013, continuously updated).

Morphological descriptions are based on notes taken from fresh collections and associated photographs, dried fungarium specimens, and other sequenced material. Micromorphological examination followed Miller et al. (2020). The following were calculated for ascospore lengths and widths for each specimen: the range in minimum and maximum values, the mean length (L_m), mean width (W_m), length-width ratio (Q), and mean length-width ratio (Q_m). The lengths of the ascospore apiculi are included in the measurements of ascospore length. Small fragments of the hymenial layer were rehydrated in 5% KOH, washed in distilled water, and sections were prepared at 25 μm thickness using a Physitemp BSF-3 freezing stage mounted on a Leica SM2000 sliding microtome. Images of micromorphological features were captured with an Olympus DP22 digital camera mounted on a BX52 compound microscope using Olympus Imaging Software Cell^D and processed using Adobe Photoshop 2021 (Adobe Systems Inc., Mountain View, California).

The following specimens were examined and annotated: *G. americanigigas* (CUP-A-024034, CUP-070734, MICH352014, MICH352015, MICH352016, MICH352017, MIN890906), *G. gigas* (ILLS00121401, NY01943083, O174609, OULU F25301, YSU-F-11757, YSU-F-11758), and *G. ussuriensis* (CUP-JA-000675, TAAM060483, YSU-F-08006). Voucher specimen number, locality, GenBank accession numbers, and source for all taxa included in the ITS and LSU analyses are shown in Table 1.

Molecular data

Methods for the extraction, PCR amplification, and sequencing of the internal transcribed spacer (ITS) region and the first 600 bp of the 5' end of 28S nuclear ribosomal large subunit (LSU) followed Miller et al. (2020). Sequences were produced at the Roy J. Carver Biotechnology Center at the University of Illinois Urbana-Champaign, and consensus sequences were assembled with Sequencher 5.4 (Gene Codes Corp., Ann Arbor, Michigan, USA).

Phylogenetic analyses

ITS and LSU datasets were individually aligned using MUSCLE® as implemented in Sequencher 5.4. Since most taxa had missing data in the two datasets, portions of the 5' and 3' ends were excluded from all analyses. Both the ITS and LSU datasets possessed little sequence variation in their final alignments so removal of ambiguously aligned regions was unnecessary. The ITS and LSU alignments are included as FASTA-formatted files (Supplementary). Both ITS and LSU alignments were rooted with *G. montana* based on previous analyses (Miller et al. 2020). The Hasegawa-Kishino-Yano (HKY) model (Hasegawa et al. 1985) was determined to be the best-fit model for both datasets by jModeltest (Darriba et al. 2012; Guindon and Gascuel 2003) based on the Akaike information criterion (AIC) (Posada and Buckley 2004). A maximum likelihood (ML) analysis with the HKY model and all parameters optimized was performed with 1000 bootstrap replicates using PhyML as implemented in Seaview 4.7 (Gouy et al. 2010). An additional ML analysis with a GTRCAT approximation and 1000 bootstrap replicates employing GAMMA model of rate heterogeneity and the rapid bootstrapping option (Stamatakis et al. 2008) was also performed using RAxML-HPC2 v.8.2.12 (Stamatakis 2014) in the CIPRES Science Gateway v.3.3 portal (Miller et al. 2010). Clades with bootstrap values (BV) ≥ 70% were considered significant and supported (Hillis and Bull 1993). Bayesian analyses were performed under the above model using MrBayes v 3.2.7 (Huelsenbeck and Ronquist 2001, 2005) on the CIPRES 3.3 portal. The Bayesian analyses were run for 1,000,000 generations which was when the average standard deviation of split frequencies was below 0.01 with trees saved every 1000 generations and burn-in set at 25%. Bayesian posterior probabilities (BPP) were determined from

Table 1 Specimens used in this study including type designation, voucher specimen number, locality, ITS and LSU GenBank accession numbers, and source of sequences. Newly generated sequences are in boldface

Species	Voucher specimen no.	Locality	ITS GenBank no.	LSU GenBank no.	Source
Gyromitra americanigigas					
	MICH 352017	**Canada: New Brunswick**	**ON527892**	**ON532828**	**This study**
	MICH 24092	**Canada: Nova Scotia**	**ON527893**	**ON532829**	**This study**
HOLOTYPE	**MICH 352014**	**USA: Michigan**	**ON527894**	**ON532830**	**This study**
	MICH 352015	**USA: Michigan**	**ON527895**	**ON532831**	**This study**
	MICH 352016	**USA: Michigan**	**ON527896**	**ON532832**	**This study**
	NY 01797009	**USA: Michigan**	**ON527897**	KC751519	**This study**
	MIN890906	USA: Minnesota	MT373909	– – – – – –	Healy unpublished
	BPI 895482	**USA: New Hampshire**	**ON527898**	– – – – – –	**This study**
	CUP-A-024034	**USA: New York**	**ON527899**	– – – – – –	**This study**
	CUP-070734	**USA: New York**	**ON527900**	**Deposited as ITS-LSU**	**This study**
	F-C0228434F	**USA: Wisconsin**	**ON527901**	– – – – – –	**This study**
Gyromitra gigas					
	NY 01943083	**Austria**	**ON527902**	– – – – – –	**This study**
EPITYPE	TUR-A 208088	Czech Republic	MH938663	MH938309	Carbone et al. 2018
	TAAM190163	Estonia	MW076963	MW076976	Miller et al. 2020
	TAAM040189	**Estonia**	**ON527903**	**ON532833**	**This study**
	TAAM060481	**Estonia**	**ON527904**	– – – – – –	**This study**
	TAAM072130	**Estonia**	**ON527905**	– – – – – –	**This study**
	TAAM076736	**Estonia**	**ON527906**	– – – – – –	**This study**
	TAAM040364	**Estonia**	– – – – – –	**ON532834**	**This study**
	TU117077	Estonia	UDB020355	UDB020355	Tedersoo et al. Global soil samples
	G4178	Estonia	UDB0485039	– – – – – –	Tedersoo et al. Global soil samples
	G4382	Estonia	UDB0435061	– – – – – –	Tedersoo et al. Global soil samples
	G4390	Estonia	UDB0466718	– – – – – –	Tedersoo et al. Global soil samples
	G4510	Estonia	UDB0392834	– – – – – –	Tedersoo et al. Global soil samples
	G4626	Estonia	UDB0327095	– – – – – –	Tedersoo et al. Global soil samples
	G4627	Estonia	UDB0337494	– – – – – –	Tedersoo et al. Global soil samples
	G4768	Estonia	UDB0483315	– – – – – –	Tedersoo et al. Global soil samples
	G4813	Estonia	UDB0192402	– – – – – –	Tedersoo et al. Global soil samples
	OULU-F 23717; ILLS00121402	Finland	MW076967	MW076977	Miller et al. 2020
	OULU-F 23577; ILLS00121403	Finland	– – – – – –	MW076978	Miller et al. 2020
	OULU-F 25304; ILLS00121404	Finland	– – – – – –	MW076979	Miller et al. 2020
	OULU-F 25301; ILLS00121405	Finland	MW076968	MW076980	Miller et al. 2020
	LY NV 2007.04.20	France	MH938665	MH938311	Carbone et al. 2018

Table 1 (continued)

Species	Voucher specimen no.	Locality	ITS GenBank no.	LSU GenBank no.	Source
	HMAS254604; ILLS00121400	France	MG846996	MG847005	Wang and Zhuang 2019
	ILLS00121401	France	MW076969	MW076969	Miller et al. 2020
	ILLS00121407	France	MW076970	MW076970	Miller et al. 2020
	ILLS00121408	France	MW076971	MW076971	Miller et al. 2020
	ILLS00121409	France	MW076972	– – – – – –	Miller et al. 2020
	ILLS00121410	France	MW076973	– – – – – –	Miller et al. 2020
	ILLS00121411	France	MW076974	MW076974	Miller et al. 2020
	LK95 04 08	Hungary	MH938664	MH938310	Carbone et al. 2018
	TUR-A 208089	Italy	MH938666	– – – – – –	Carbone et al. 2018
	TUR-A 208091	Italy	MH938667	MH938312	Carbone et al. 2018
	TUR-A 208092	Italy	MH938668	MH938313	Carbone et al. 2018
	TUR-A 208093	Italy	MH938669	MH938314	Carbone et al. 2018
	14754	Italy	JF908781	– – – – – –	Osmundson et al. 2013
	O174609	Norway	MW076964	KX008328	Miller et al. 2020
	O174628	Norway	MW076965	KX008329	Miller et al. 2020
	O174629	Norway	MW076966	KX008330	Miller et al. 2020
	LE-F-333107	**Russia: Kemerovo Oblast**	**ON527907**	– – – – – –	**This study**
	YSU-F-11757	**Russia: Kemerovo Oblast**	**ON527908**	**ON532835**	**This study**
	LE 215221	**Russia: Leningrad Oblast**	**ON527909**	– – – – – –	**This study**
	LE 247133	**Russia: Leningrad Oblast**	**ON527910**	– – – – – –	**This study**
	LE 247586	**Russia: Leningrad Oblast**	**ON527911**	– – – – – –	**This study**
	LE 294463	**Russia: Novgorod Oblast**	**ON527912**	– – – – – –	**This study**
	YSU-F-11758	**Russia: Novosibirsk Oblast**	**ON527913**	**ON532836**	**This study**
	LE 247628	**Russia: Pskov Oblast**	**ON527914**	– – – – – –	**This study**
	LE 247629	**Russia: Pskov Oblast**	**ON527915**	– – – – – –	**This study**
	H.546	Turkey	KX420694	– – – – – –	Gungor et al. unpublished
	H.559	Turkey	KX420695	– – – – – –	Gungor et al. unpublished
	H.815	Turkey	KX420696	– – – – – –	Gungor et al. unpublished
Gyromitra montana					
	DAOM 706056; ILLS00121424	Canada: Newfoundland	MW077459	MW077445	Miller et al. 2020
ISOTYPE	BPI 566707	USA: Wyoming	MW077452	MW077442	Miller et al. 2020
Gyromitra ussuriensis					
	HMAS89008	China: Jilin	MG846995	MG847004	Wang and Zhuang 2019
	TNS-F-15631	**Japan: Hokkaido**	**ON527916**	– – – – – –	**This study**
	TNS-F-31137	**Japan: Ibaraki**	**ON527917**	**ON532837**	**This study**
	CUP-JA-000675	**Japan: Ishikari**	**ON527918**	– – – – – –	**This study**
	TNS-F-17980	**Japan: Tochigi**	**ON527919**	– – – – – –	**This study**
	TNS-F-66010	**Japan: Tochigi**	**ON527920**	**ON532838**	**This study**
	TNS-F-66526	**Japan: Tochigi**	**ON527921**	– – – – – –	**This study**
	YSU-F-08006; ILLS00121415	Russia: Khanty-Mansiysky Autonomous Okrug	MW076975	MW076981	Miller et al. 2020
NEOTYPE	**TAAM060483**	**Russia: Primorsky Kray**	**ON527922**	– – – – – –	**This study**
	LE 304601	**Russia: Siberia, Krasnoyarsky Krai**	**ON527923**	– – – – – –	**This study**
	LE 304603	**Russia: Siberia, Krasnoyarsky Krai**	**ON527924**	– – – – – –	**This study**
	LE 323486	**Russia: Siberia, Krasnoyarsky Krai**	**ON527925**	– – – – – –	**This study**
	KH:KA19-0027	South Korea	MZ567190	MZ573189	Cho et al. 2021

Table 1 (continued)

Species	Voucher specimen no.	Locality	ITS GenBank no.	LSU GenBank no.	Source
	KH:KA21-0152	South Korea	MZ567197	MZ573196	Cho et al. 2021
	KH:KA19-0153	South Korea	MZ567198	MZ573197	Cho et al. 2021

a consensus tree using PAUP* 4.0b10 (Swofford 2002), and clades with BPP ≥ 95% were considered significant and strongly supported (Alfaro et al. 2003; Larget and Simon 1999).

Sequence similarity comparisons

Comparisons between ITS and LSU sequences and between the ITS1 and ITS2 regions were made in PAUP v.4.0a (build 166) (Swofford 2002) with distance set to uncorrected "p." Mean and range were calculated for infraspecific and interspecific variation. The ITS1 and ITS2 regions were delimited using the ITSx program in PlutoF (Abarenkov et al. 2010).

Results

Phylogenetic analyses

PCR amplification and Sanger sequencing of ITS and LSU were largely successful from DNA extracted from most specimens, even those over 60 years old (Table 1). The final ITS alignment of 75 sequences consisted of 738 nucleotides after the removal of nucleotides on the 5' and 3' ends due to missing characters in most taxa. No ambiguously aligned characters occurred in the ITS alignment. The ITS contained 49 parsimony-informative characters with gaps treated as missing characters: 34 in the ITS1 region and 15 in the ITS2 region.

The final LSU alignment of 40 sequences consisted of 864 nucleotides after the removal of nucleotides on the 5' and 3' ends due to missing characters in most taxa. No ambiguous regions were present in the LSU dataset. The LSU contained only 3 parsimony-informative characters and lacked sufficient phylogenetic signal to differentiate among these putative taxa (data not shown) so phylogenetic relationships are based only on the ITS dataset.

Analyses of the ITS dataset generated identical most-likely trees in both the PhyML and RAxML analyses, except BV were higher in the RAxML tree (Fig. 1). Three distinct, well-supported monophyletic clades were formed that corresponded to three closely related, but separate species. *Gyromitra gigas* formed a highly supported clade with 90% BV and significant BPP. The clade containing members of *G. ussuriensis* was supported with 70% BV and significant BPP. The new species, *G. americanigigas*, is well-supported with 96% BV, but without significant BPP. *Gyromitra gigas* and *G. ussuriensis* occurred as sister taxa in a clade supported by significant BPP.

Distribution

Each of these three species inhabits a specific geographic region with some overlap in central Russia between *G. gigas* and *G. ussuriensis* (Fig. 2). All known species in the *G. gigas* species complex are shown on the map for clarity. *Gyromitra americanigigas* occurs throughout northeastern USA and southeastern Canada. Its range overlaps with *G. korfii* in Michigan and New York and with *G. montana* in Michigan and Canada. *Gyromitra gigas* occupies a large range extending from western Europe to central Russia and overlaps with *G. ticiniana* in France, Italy, and Turkey and with *G. ussuriensis* in central Russia. *Gyromitra ussuriensis* occurs mostly in eastern China, Japan, eastern Russia, and South Korea. *Gyromitra khanspurensis* is known only from its type locality in Pakistan, whereas *G. pseudogigas* has only been collected in Sichuan Province of China.

Taxonomy

Gyromitra americanigigas Dirks, A.N. Mill. & Methven, sp. nov. Fig. 3

MycoBank: MB844178

Type: USA, Michigan, Washtenaw County, Stinchfield Woods, 42.41 N, 83.92 W, on soil in a *Pinus* sp. plantation, 5 May 2020, A.C. Dirks (ACD0256), Holotype (MICH352014), Isotype (ILLS00114755), GenBank ON527894 (ITS), GenBank ON532830 (LSU).

Etymology: Named for the combination of "americana" and "gigas" to describe this new species from North America that is closely related to the European *G. gigas*.

Description: Ascomata consisting of an apical hymenophore and stipe, 5–12 cm high. Hymenophore 2–6 cm high, 5–9 cm diam., convoluted and folded; hymenium pruinose, brownish orange to brown; margin free; sterile surface smooth, tan. Stipe 3–6 cm long, 2–5 cm diam., off-white, longitudinally wrinkled and pitted, hollow. Excipulum one-layered, of *textura intricata*, hyaline. Paraphyses cylindric, apices clavate, inflated up to 7.5–10 μm diam., thin-walled, septate, unbranched, golden-brown in

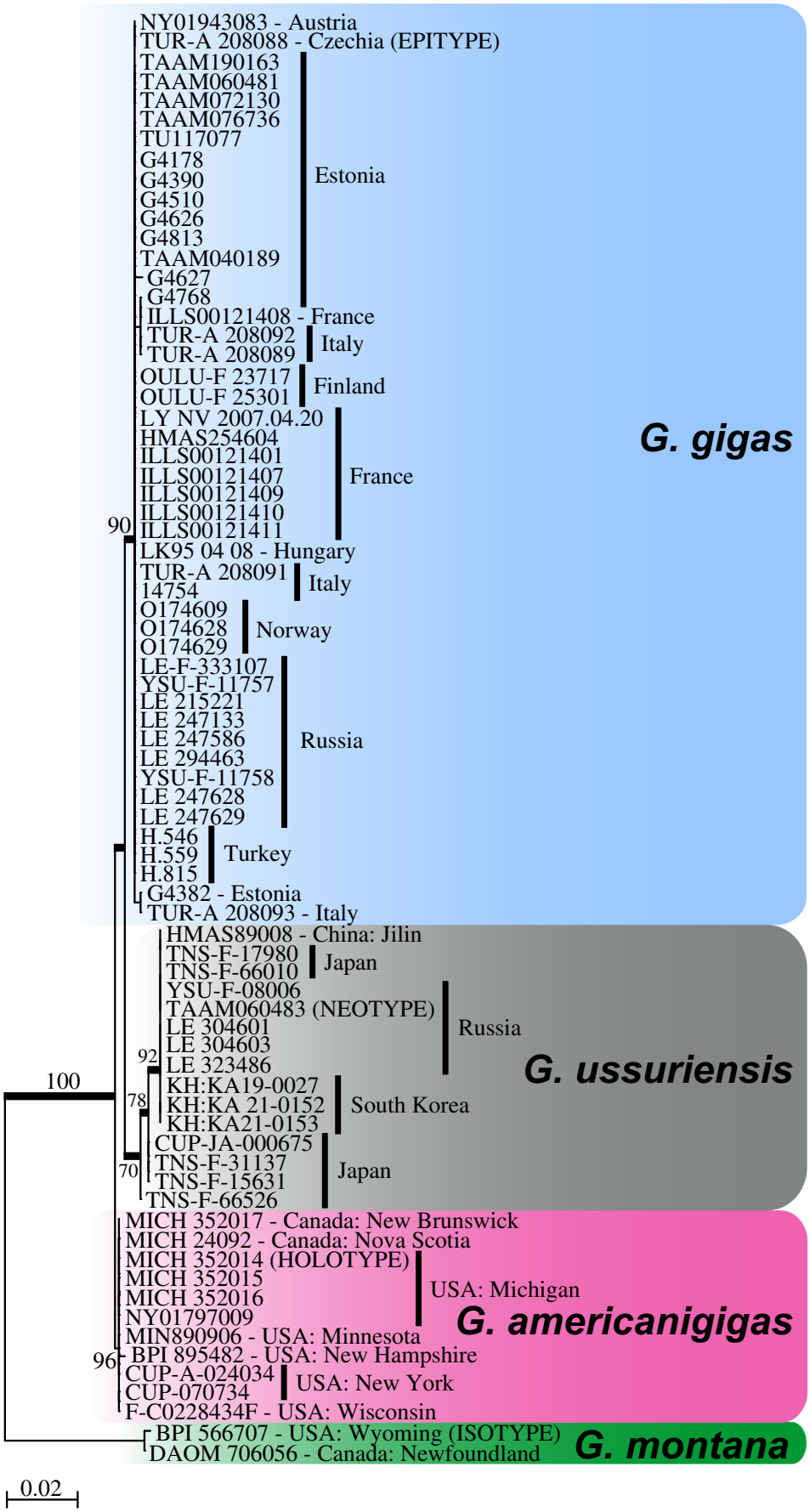
NY01943083 - Austria
TUR-A 208088 - Czechia (EPITYPE)
TAAM190163
TAAM060481
TAAM072130
TAAM076736
TU117077
G4178
G4390
G4510
G4626
G4813
TAAM040189
G4627
G4768
Estonia
ILLS00121408 - France
TUR-A 208092
TUR-A 208089
Italy
OULU-F 23717
OULU-F 25301
Finland
LY NV 2007.04.20
HMAS254604
ILLS00121401
ILLS00121407
ILLS00121409
ILLS00121410
ILLS00121411
France
90
LK95 04 08 - Hungary
TUR-A 208091
14754
Italy
O174609
O174628
O174629
Norway
LE-F-333107
YSU-F-11757
LE 215221
LE 247133
LE 247586
LE 294463
YSU-F-11758
LE 247628
LE 247629
Russia
H.546
H.559
H.815
Turkey
G4382 - Estonia
TUR-A 208093 - Italy
G. gigas
HMAS89008 - China: Jilin
TNS-F-17980
TNS-F-66010
Japan
YSU-F-08006
TAAM060483 (NEOTYPE)
LE 304601
LE 304603
LE 323486
Russia
92
KH:KA19-0027
KH:KA 21-0152
KH:KA21-0153
South Korea
100
78
CUP-JA-000675
TNS-F-31137
TNS-F-15631
TNS-F-66526
Japan
70
G. ussuriensis
MICH 352017 - Canada: New Brunswick
MICH 24092 - Canada: Nova Scotia
MICH 352014 (HOLOTYPE)
MICH 352015
MICH 352016
NY01797009
MIN890906 - USA: Minnesota
USA: Michigan
BPI 895482 - USA: New Hampshire
96
CUP-A-024034
CUP-070734
USA: New York
F-C0228434F - USA: Wisconsin
G. americanigigas
BPI 566707 - USA: Wyoming (ISOTYPE)
DAOM 706056 - Canada: Newfoundland
G. montana
0.02

◀ **Fig. 1** RAxML phylogram inferred from ML and Bayesian analyses of 75 ITS sequences from type and voucher specimens of *Gyromitra americanigigas*, *G. gigas*, and *G. ussuriensis*. *Gyromitra montana* is used as an outgroup. Specimen numbers are given followed by country and state/province. Type specimens for each species are given in parentheses. RAxML bootstrap support values above 70% are shown at the nodes, and Bayesian posterior probability scores above 0.95 are shown as thickened branches

KOH. Asci 275–325 × 17.5–20 µm, cylindric, operculate, thin-walled, hyaline, eight-spored. Ascospores uniseriate, 28–34 × 10–12 µm (L_m 30.3 µm, W_m = 11.0 µm, Q = 2.3–3.0, Q_m = 2.8), ellipsoid to fusoid, at times inequilateral; surface finely wrinkled; apiculi knob-like, 2–3 µm long; perispore up to 1 µm thick, cyanophilic; content triguttulate, with one large central oil drop and two smaller polar oil drops, hyaline. Ascospores white in mass.

Ecology and distribution: Solitary to scattered on soil and wood in temperate coniferous and deciduous-coniferous forests in May. Known from New Brunswick and Nova Scotia in Canada and from Michigan, Minnesota, New York, and Wisconsin in USA.

Notes: *Gyromitra americanigigas* is macro- and micromorphologically similar to *G. gigas*, *G. korfii*, and *G. montana*. *Gyromitra gigas*, which is restricted to Europe and Asia, has slightly broader ascospores at 12–13(14) µm (Carbone et al. 2018). *Gyromitra korfii*, which also occurs in eastern North America, has longer ascospores ((29.2)31.5–37(37.3) × (9.7)10.4–10.9(12) µm; Raitviir 1970) and more prominent apiculi. *Gyromitra montana*, which occurs in western North America and Canada, has ascospores that measure (21.4)24.3–35.8(37.5) × (9)10.7–15.8 µm with shorter apiculi (0.1–1 µm) (McKnight 1971).

Additional specimens examined: CANADA, New Brunswick, Albert, 45.88 N, 64.82 W, on soil in mixed forest of balsam fir, birch, aspen, ash, and maple, 4 May 2021, T. Gilchist (ACD0418, MICH352017) (immature); USA, Michigan, Washtenaw County, Stinchfield Woods, 42.41 N, 83.92 W, on and at base of pine in conifer plantation, 5 May 2020, A.C. Dirks (ACD0257, MICH352015); on soil and dead conifer wood in conifer plantation, 5 May 2020, A.C. Dirks (ACD0258, MICH352016); Minnesota, Saint Louis County, Duluth, Lester State Park, off Seven Bridges Road, on buried wood underneath dead spruce in mixed spruce, aspen, birch forest, 29 May 2003, B.T. Dentinger (BD179, MIN890906); New York, Tompkins County, Dryden, Observation Hill, McLean Moor, 42.65 N, 76.29 W, in mossy ground, 26 May 1917, V. Dunlap (CUP-A-024034); Tioga County, Spencer, 42.21 N, 76.49 W, 3 May 2019, A. Schmalfuss (CUP-070734) (immature).

Gyromitra ussuriensis Lj.N. Vassiljeva Fig. 4

MycoBank: MB298070

Typification: Neotype: RUSSIA, Primorsky Kray, Ussurisky Nature Reserve [formerly Suputinsky Nature Reserve], on base of deciduous tree trunk, 2 Jun 1961, L.N. Vassiljeva (*Neotype designated here* TAAM 060483; MBT10007298), GenBank ON527922 (ITS2).

Fig. 2 Distribution map for all eight species in the *G. gigas* species complex. Type specimens for each species are shown as stars, and sequenced voucher specimens are shown as circles. Colors for each species are shown in the legend

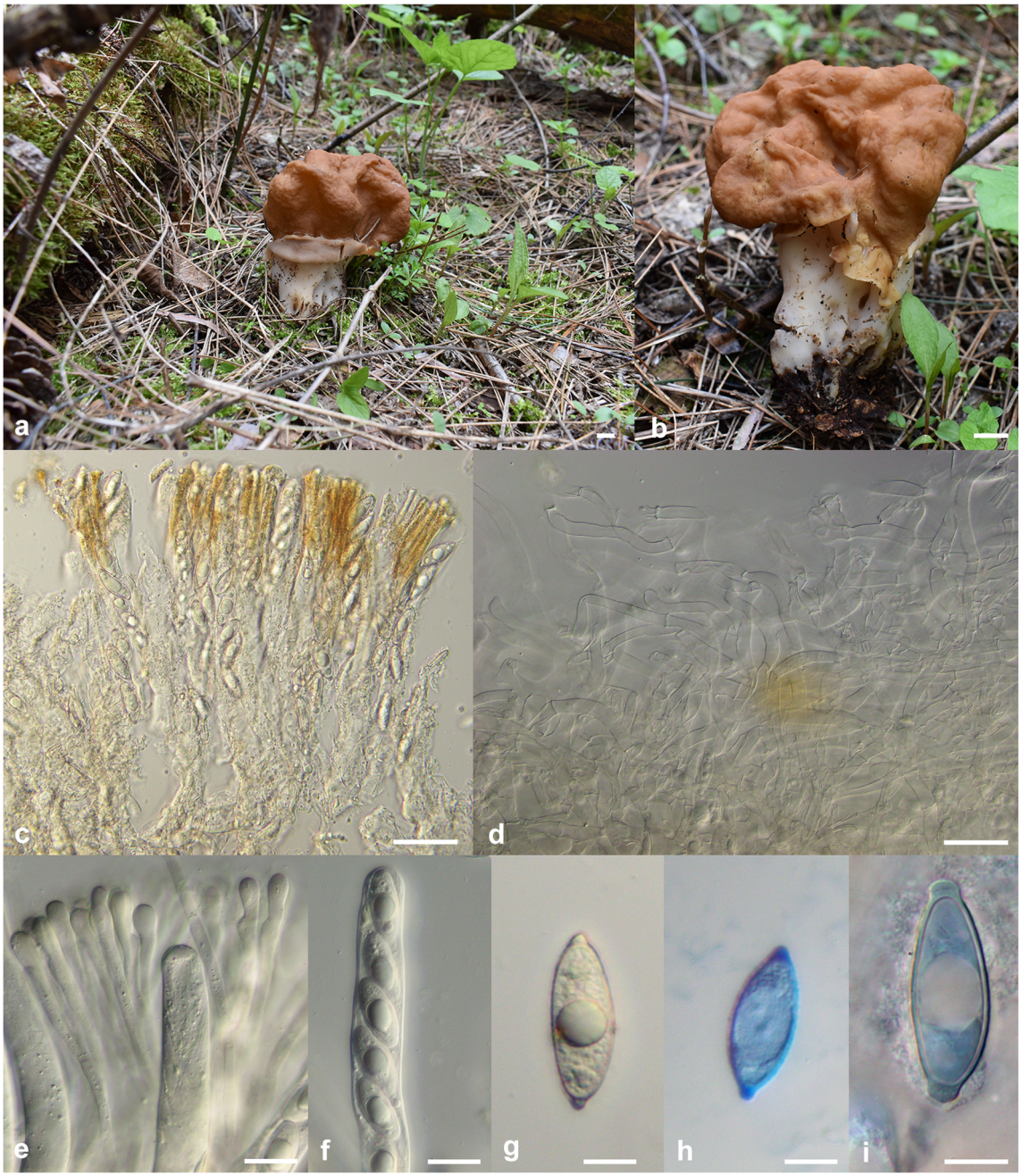

Fig. 3 *Gyromitra americanigigas* (MICH352014, holotype). **a**, **b** Single ascocarp (bar = 1 cm), **c** hymenial layer showing asci and paraphyses with golden brown apices (bar = 50 μm) (BF), **d** excipulum composed of *textura intricata* (bar = 50 μm) (DIC), **e** paraphyses apices (bar = 20μm) (DIC), **f** ascus with immature ascospores (bar = 20 μm) (DIC), **g**–**i** ascospores (DIC), **h**–**i** ascospores stained with lactophenol in cotton blue (bar = 10 μm)

Holotype (from Vassiljeva 1950): USSR: Extremus Oriens, distr. Voroschilov in valle fl. Suputinka, ad truncos putridos *Betulae* et *Pini korajensis*, V 1946, leg. auctor; distr. Schkotovo, Maiche-Daubiche plato, ad truncos putridos *Betulae costatae*, VI 1947, leg. B.P. Kolesnikov et V.A. Rosenberg.

Description: Ascomata consisting of an apical hymenophore and stipe, 9–16 cm high. Hymenophore 4–10 cm diam., inflated, plicate-lobate, deformed; hymenium brown to ochraceous-brown; margin free. Stipe 4–10 cm long × 2–6 cm diam., white, longitudinally wrinkled and pitted, hollow. Excipulum one-layered, of *textura intricata*, hyaline. Paraphyses cylindric, apically clavate, inflated up to 7–10 μm, thin-walled, septate, unbranched, yellow-brown in KOH. Asci 250–325 × 17.5–20 μm, operculate, thin-walled, cylindric, hyaline, eight-spored. Ascospores uniseriate, (27)28–

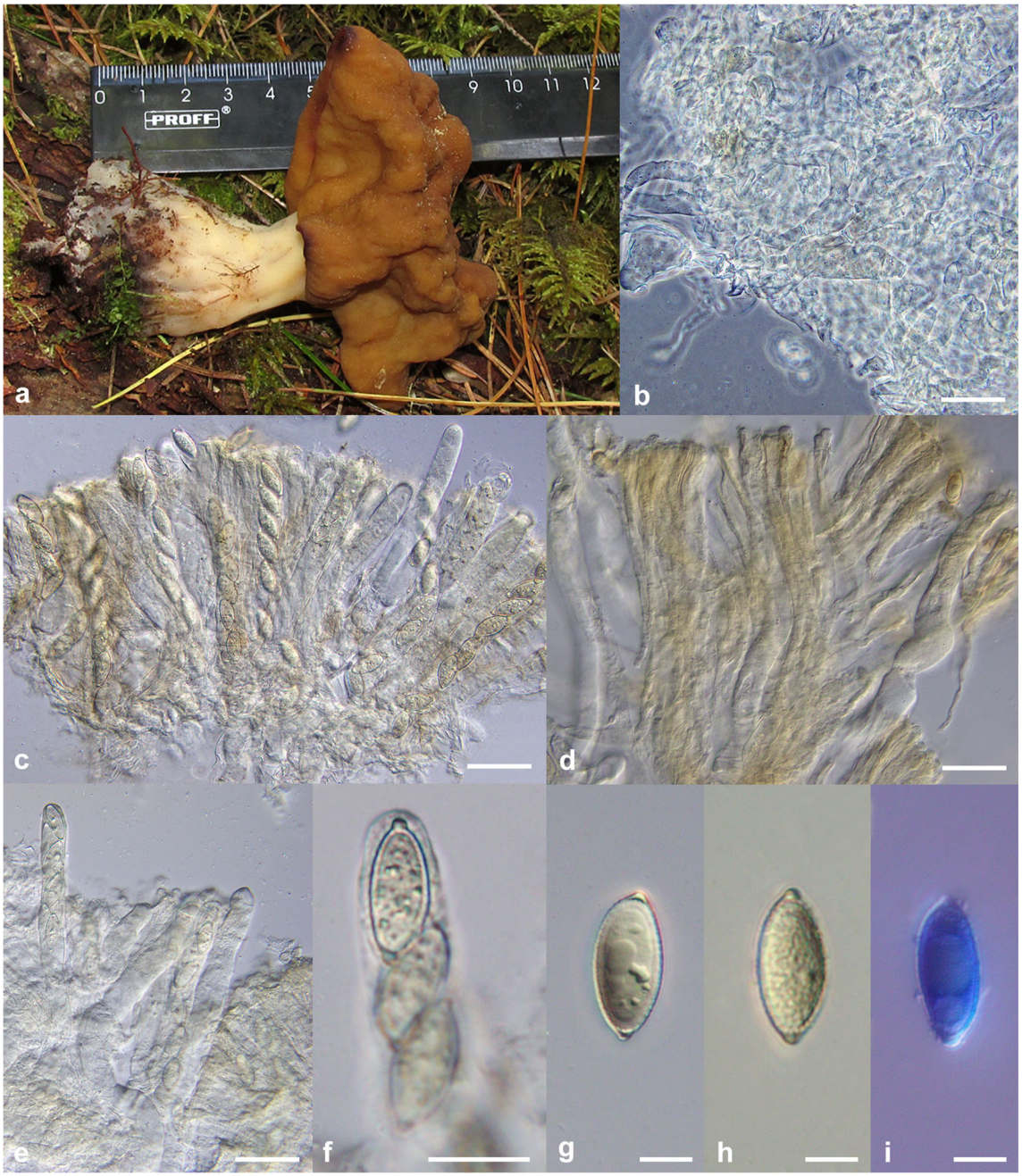

Fig. 4 *Gyromitra ussuriensis* (TAAM060483, neotype, except a from LE 304603). **a** Ascocarp growing on decaying spruce wood, **b** excipulum composed of *textura intricata* (bar = 50 μm) (DIC), **c** hymenial layer showing asci and paraphyses (bar = 50 μm) (DIC), **d** paraphyses with golden brown apices (bar = 50 μm) (DIC), **e** asci with immature ascospores (bar = 50 μm) (DIC), **f** ascus apex (bar = 20 μm) (DIC), **g**–**i** ascospores (DIC), **i** ascospore stained with lactophenol in cotton blue (bar = 10 μm)

32(33) × 12–13 μm (L_m = 29.5 μm; W_m = 12.5 μm; Q = 2.2–2.6; Q_m = 2.4), ellipsoid to fusoid; surface roughened; apiculi knob-like, up to 2.5 μm long; perispore up to 1 μm thick, cyanophilic; content triguttulate, with one large central oil drop and two smaller polar oil drops, hyaline.

Ecology and distribution: Solitary to scattered on soil or decayed wood of *Betula*, *Picea*, *Pinus korajensis*, and *Populus tremula* in temperate coniferous and deciduous-coniferous forests in May and June. Known from eastern China, Japan, South Korea, and central and eastern Russia.

Notes: *Gyromitra ussuriensis* is similar to *G. gigas*, and several researchers (Raitviir 1970; Van Vooren and Moreau 2009; Carbone et al. 2018) have placed *G. ussuriensis* in synonymy with *G. gigas*. However, molecular data supports recognition of *G. ussuriensis* as a distinct species. Vassiljeva (1950) described the ascospores as "33–40 × 11–13 μm,

broadly fusiform; surface rugose-tuberculate, hyaline to pale brown." She also stated that *G. ussuriensis* is distinguished from *G. gigas* by the "smaller hymenophore that has a free margin, long stipe, and growth on wood." The epitype of *G. gigas* selected by Carbone et al. (2018) is similar macromorphologically and micromorphologically to *G. ussuriensis*. Carbone et al. (2018) described the ascospores of the epitype of *G. gigas* as "(25)27–32(34.5) × (11.5)12–13(14) μm on free spores [the most frequent 27–30 × 12–13 μm], Q = (2.1)2.2–2.5(2.75)."

The holotype specimen at VLA is missing and presumably lost, and no original material or illustration exists (Eugenia Bulakh, pers. comm.). Therefore, a specimen collected by Vassiljeva from the same locality as the holotype is designated as neotype here (TAAM060483). This specimen also happens to be the same specimen that Raitviir examined when he synonymized *G. ussuriensis* under *G. gigas* (Raitviir 1970). This neotype specimen has been sequenced for the ITS2 region using Illumina next-generation sequencing (Miller et al. 2022). A video of the discovery of YSU-F-08006 is also available at https://youtu.be/Jq0WV67-crA.

Other specimens examined: JAPAN, Ishikari, Hokkaido, Toyohiracho, Jozankei, 42.94 N, 141.13 E, 18 May 1958, S. Kamei, T. Yokoyama, R.P. Korf (CUP-JA-000675) (immature), RUSSIA, Khanty-Mansiysky Autonomous Okrug, Khanty-Mansiysky Rayon, Shapsha village, 61.08 N, 69.45 E, on large dead aspen (*Populus tremula*) log, 26 Jun 2018, N. Filippova (YSU-F-08006, ILLS00121415).

Sequence similarity comparisons

The ITS region was compared to LSU to investigate the infraspecific and interspecific variability of these two common molecular markers. Infraspecific ITS sequence variation on average was zero in *G. americanigigas* and *G. gigas* and 0.1% in *G. ussuriensis* (Table 2). Infraspecific LSU sequence variation on average was zero in all three species. Interspecific ITS sequence variation on average ranged from 0.7% between *G. americanigigas* and *G. gigas* to 1.2% between *G. americanigigas* and *G. ussuriensis*. This is compared to 5.6–6.5% sequence variation between these three species and *G. montana*. Interspecific LSU sequence variation on average ranged from zero between *G. americanigigas* and *G. ussuriensis* to 0.1% between the other two combinations. Sequence variation was equally low ranging from 0.2 to 0.4% between the three target species and *G. montana*. Whereas the ITS displayed a significant barcode gap and can be used to recognize these three species, the LSU had no barcode gap with infra- and interspecific variation nearly identical.

The ITS1 and ITS2 regions were compared to determine whether either one of these two regions could be used as a barcode marker for molecular identification of these taxa as is the case for most environmental sampling studies (Table 3). Infraspecific sequence variation in the ITS1 ranged between 0 and 0.3% and averaged 0–0.1%. Infraspecific sequence variation in the ITS2 ranged between 0 and 0.7% and averaged 0–0.1%. The ITS1 region contained more than twice the number of parsimony-informative characters compared to the ITS2

Table 2 Infraspecific and interspecific sequence variation of the ITS and LSU for *G. americanigigas*, *G. gigas*, *G. ussuriensis*, and the outgroup, *G. montana*. Mean and range (in parentheses) of percent differences based on uncorrected "p" sequence differences are shown for ITS along the upper diagonal and for LSU along the lower diagonal

	G. americanigigas	*G. gigas*	*G. ussuriensis*	*G. montana*
G. americanigigas	ITS = 0 (0 – 0.3) LSU = 0 (0 – 0.2)	0.7 (0 – 1.0)	1.2 (0.9 – 1.7)	5.6 (3.4 – 6.4)
G. gigas	0.1 (0 – 0.3)	ITS = 0 (0 – 0.3) LSU = 0 (0 – 0.5)	1.0 (0 – 1.4)	6.5 (3.3 – 9.1)
G. ussuriensis	0 (0 – 0)	0.1 (0 – 0.3)	ITS = 0.1 (0 – 0.7) LSU = 0 (0)	6.1 (3.5 – 6.6)
G. montana	0.2 (0.2 – 0.3)	0.4 (0.2 – 0.7)	0.2 (0.2 – 0.3)	ITS = 0 (0 – 0.1) LSU = 0 (0)

Table 3 Infraspecific and interspecific sequence variation of the ITS1 and ITS2 regions for *G. americanigigas*, *G. gigas*, *G. ussuriensis*, and the outgroup, *G. montana*. Mean and range (in parentheses) of percent differences based on uncorrected "p" sequence differences are shown for ITS1 along the upper diagonal and for ITS2 along the lower diagonal

	G. americanigigas	*G. gigas*	*G. ussuriensis*	*G. montana*
G. americanigigas	ITS1 = 0 (0 – 0) ITS2 = 0 (0 – 0.3)	0.9 (0.9 – 1.3)	0.9 (0.9 – 1.1)	9.5 (8.9 – 10.3)
G. gigas	0.6 (0.5 – 1.1)	ITS1 = 0 (0 – 0.3) ITS2 = 0.1 (0 – 0.5)	1.2 (1.2 – 1.9)	10.3 (9.8 – 10.7)
G. ussuriensis	1.3 (0.8 – 1.7)	0.7 (0 – 1.4)	ITS1 = 0 (0 – 0) ITS2 = 0.1 (0 – 0.7)	10.1 (9.5 – 11.9)
G. montana	3.3 (3.2 – 3.5)	3.2 (3.2 – 3.5)	3.1 (2.9 – 3.6)	ITS1 = 0.1 (0 – 0.3) ITS2 = 0 (0 – 0)

region (34 vs. 15), and thus, it was expected that, in general, the ITS1 would vary twice as much as the ITS2. Interspecific variability was three times higher in the ITS1 versus the ITS2 region in comparisons of *G. montana* to the three target species, a result consistent with our previous findings (Miller et al. 2020). Interspecific ITS1 sequence variation on average ranged from 0.9% between *G. americanigigas* and *G. gigas* (and 0.9% between *G. americanigigas* and *G. ussuriensis*) to 1.2% between *G. gigas* and *G. ussuriensis*. Interspecific ITS2 sequence variation on average ranged from 0.6% between *G. americanigigas* and *G. gigas* to 1.3% between *G. americanigigas* and *G. ussuriensis*. Whereas infraspecific variation averaged less than 0.1%, interspecific variation averaged 0.6–1.3% for all three species comparisons. The ITS1 and ITS2 regions both displayed similar sequence variability among these three species, justifying the use of either the ITS1 or ITS2 region or both as a molecular barcode marker for species identification.

Species concepts

Species within the *G. gigas* monophyletic group are characterized by stipitate ascomata, hymenophores that are saddle-shaped to irregularly lobed or cerebriform and wrinkled, and yellow-brown to brown to reddish brown, ribbed to sulcate, white to yellow-brown stipe, ellipsoid to fusiform ascospores that are roughened to finely reticulate and uniguttulate or triguttulate with inconspicuous to distinctive single apiculi that are up to 4 μm long. Although we attempted to apply a polyphasic approach to species delimitation, our morphological examination revealed no significant characters to distinguish *G. americanigigas*, *G. gigas*, and *G. ussuriensis*. However, there appears to be some geographical signal to the speciation that has occurred in this group (Fig. 2). Attempts to culture species in the *G. gigas* complex failed, and we are unaware of anyone else successfully doing so (Healy et al. 2022), preventing the use of intercompatibility tests to facilitate the delimitation of species boundaries under the biological species concept. The LSU cannot be used as a barcode marker since the infra- and interspecific variation among sequences of these three species was nearly identical. However, the ITS does contain an adequate barcode gap and can be used for species identification of these three species using a phylogenetic species concept.

Discussion

Although species concepts in the *Gyromitra gigas* species complex were believed to be resolved (Miller et al. 2020), some secrets still remained due to cryptic speciation. Three well-supported clades representing *G. gigas*, a new species (*G. americanigigas*), and a rediscovered species (*G. ussuriensis*) were revealed in our phylogenetic analyses (Fig. 1). Unfortunately, these three species do not possess any significant differences by which to delimit them morphologically. Although Vassiljeva (1950) originally described the ascospores of *G. ussuriensis* as being longer than in *G. gigas*, we could not confirm her results. She also distinguished it from *G. gigas* as having a smaller hymenophore with a free margin, long stipe, and growth on wood, but these characters are also

shared by *G. gigas* (Carbone et al. 2018). However, these three species do occupy somewhat distinct geographical areas with *G. americanigigas* confined to Canada and USA, *G. gigas* occurring mostly in Europe, and *G. ussuriensis* found in Asia (Fig. 2). Some overlap between *G. gigas* and *G. ussuriensis* does occur in central Russia, and *G. gigas* and *G. ticiniana* are both found in France, Italy, and Turkey. There is also overlap in the distributions of *G. americanigigas*, *G. korfii*, and *G. montana*, with all three species found in Michigan, USA. Sequencing of all or part of the ITS region is highly recommended for species identification in this group.

The ITS1 and ITS2 regions both display a small, but adequate barcode gap for identifying these three species either through nBLAST similarity searches or phylogenetic analyses. The infraspecific variation averaged less than 0.1%, whereas the interspecific variation averaged 0.6–1.3% for all three species comparisons. Ideally, species hypotheses should be based on ITS interspecific variation higher than 0.5–1.5%, but as more fungal species complexes are studied and more cryptic speciation is discovered, these lower percentages for species differentiation using the ITS fungal barcode may be the norm (Lücking et al. 2020). Future studies of freshly collected specimens should sequence one or more protein-coding genes, or ideally whole genomes, and use genetic discontinuity models to test our species hypotheses (Matute and Sepúlveda 2019), which would most likely corroborate our ITS data derived from mostly older fungarium specimens.

Supplementary Information The online version contains supplementary material available at https://doi.org/10.1007/s11557-022-01832-x.

Acknowledgements The authors wish to thank the curators and collection managers for the loan of specimens at the following fungaria: BPI, CUP, F, ILLS, LE, MICH, MIN, NY, O, TAAM, TNS, and YSU. Yuri Roskov at the University of Illinois is thanked for the translation of Russian text. Sanger sequencing was performed at the Roy J. Carver Biotechnology Center at the University of Illinois.

Author contribution ANM was responsible for the study conception and design. ANM, AD, and EP generated molecular sequence data. AD, EP, and NF provided voucher specimens. Molecular analyses were performed by ANM. Morphological analyses were performed by ASM. The first draft of the manuscript was written by ANM, ASM edited the manuscript, and all authors commented on subsequent versions of the manuscript. All authors read and approved the final manuscript.

Data availability All data and materials have been deposited in publicly accessible holdings.

Declarations

Ethics approval Not applicable.

Consent to participate Not applicable.

Consent for publication Not applicable.

Conflict of interest The authors declare no competing interests.

References

Abarenkov K, Tedersoo L, Nilsson RH, Vellak K, Saar I, Veldre V, Parmasto E, Prous M, Aan A, Ots M, Kurina O, Ostonen I, Jõgeva J, Halapuu S, Põldmaa K, Toots M, Truu J, Larsson KH, Kõljalg U (2010) PlutoF—a web based workbench for ecological and taxonomic research, with an online implementation for fungal ITS sequences. Evol Bioinform Online 6:189–196. https://doi.org/10.4137/EBO.S6271

Alfaro ME, Zoller S, Lutzoni F (2003) Bayes or bootstrap. A simulation study comparing the performance of Bayesian Markov chain Monte Carlo sampling and bootstrapping in assessing phylogenetic confidence. Mol Biol Evol 20:255–266. https://doi.org/10.1093/molbev/msg028

Carbone M, Van Vooren N, Klener V, Alvarado P (2018) Preliminary phylogenetic and morphological studies in the *Gyromitra gigas* lineage (*Pezizales*): Epitypification of *Gyromitra gigas* and *G. ticiniana*. Ascomycete.org 10(5):187–199. https://doi.org/10.25664/art-0241

Darriba D, Taboada GL, Doallo R, Posada D (2012) jModelTest 2: more models, new heuristics and parallel computing. Nat Methods 9:772. https://doi.org/10.1038/nmeth.2109

Gouy M, Guindon S, Gascuel O (2010) SeaView version 4: a multiplatform graphical user interface for sequence alignment and phylogenetic tree building. Mol Biol Evol 27:221–224. https://doi.org/10.1093/molbev/msp259

Guindon S, Gascuel O (2003) A simple, fast and accurate algorithm to estimate large phylogenies by maximum likelihood. Syst Biol 52:696–704. https://doi.org/10.1080/10635150390235520

Hasegawa M, Kishino H, Yano T (1985) Dating of the human-ape splitting by a molecular clock of mitochondrial DNA. J Mol Evol 22:160–174. https://doi.org/10.1007/BF02101694

Healy RA, Arnold AE, Bonito G, Huang YL, Lemmond B, Pfister DH, Smith ME (2022) Endophytism and endolichenism in *Pezizomycetes*: the exception or the rule? New Phytol 233:1974–1983

Hillis DM, Bull JJ (1993) An empirical test of bootstrapping as a method for assessing confidence in phylogenetic analysis. Syst Biol 42:182–192. https://doi.org/10.1093/sysbio/42.2.182

Huelsenbeck JP, Ronquist FR (2001) MrBayes: Bayesian inference of phylogenetic trees. Bioinformatics 17:754–755. https://doi.org/10.1093/bioinformatics/17.8.754

Huelsenbeck JP, Ronquist FR (2005) Bayesian analysis of molecular evolution using MrBayes. In: Nielsen R (ed) Statistical methods in molecular ecology. Springer Publishing Co, New York, pp 186–226

Krisai-Greilhuber I, Chen Y, Jabeen S, Madrid H, Marincowitz S, Razaq A, Ševčíková H, Voglmayr H, Yazici K, Aptroot A, Aslan A, Boekhout T, Borovička J, Crous PW, Ilyas S, Jami F, Jiang Y-L., Khalid AN, Kolecka A, Konvalinková T, Norphanphoun C, Shaheen S, Wang Y, Wingfield MJ, Wu S-P, Wu Y-M, Yu J-Y (2017) Fungal systematics and evolution: FUSE 3. Sydowia 69:229–264. https://doi.org/10.12905/0380.sydowia69-2017-0229

Larget B, Simon DL (1999) Markov Chain Monte Carlo algorithms for the Bayesian analysis of phylogenetic trees. Mol Biol Evol 16(6):750–759. https://doi.org/10.1093/oxfordjournals.molbev.a026160

Lücking R, Aime MC, Robbertse B, Miller AN, Ariyawansa H, Aoki T, Cardinali G, Crous P, Druzhinina I, Geiser D, Hawksworth D, Hyde K, Irinyi L, Jeewon R, Johnston P, Kirk P, Malosso E, May T,

Meyer W et al (2020) Unambiguous identification of fungi: where do we stand and how accurate and precise is fungal DNA barcoding? IMA Fungus 11:1–32

Matute DR, Sepúlveda VE (2019) Fungal species boundaries in the genomics era. Fungal Genet Biol 131:1–9

McKnight KH (1971) On two species of False Morels (*Gyromitra*) in Utah. Great Basin Naturalist 31(2):35–47

Miller MA, Pfeiffer W, Schwartz T (2010) Creating the CIPRES Science Gateway for inference of large phylogenetic trees. In: Proceedings of the Gateway Computing Environments Workshop (GCE), 14 Nov 2010, New Orleans, Louisiana, pp 1–8

Miller AN, Yoon A, Gulden G, Stensholt Ø, Van Vooren N, Ohenoja E, Methven AS (2020) Studies in *Gyromitra* I: the *Gyromitra gigas* species complex. Mycol Progress 19:1459–1473. https://doi.org/10.1007/s11557-020-01639-8

Miller AN, Karakehian J, Raudabaugh DB (2022) Next generation sequencing of ancient and recent fungarium specimens. J Fungi. (in press)

MyCoPortal (2022) http://mycoportal.org/portal/index.php. Accessed on March 10

Posada D, Buckley TR (2004) Model selection and model averaging in phylogenetics: advantages of Akaike information criterion and Bayesian approaches over likelihood ratio tests. Syst Biol 53:793–808. https://doi.org/10.1080/10635150490522304

Raitviir A (1970) Once more on *Neogyromitra caroliniana*. Botaanikaalased tõõd 9:364–373

Stamatakis A (2014) RAxML version 8: a tool for phylogenetic analysis and post-analysis of large phylogenies. Bioinformatics 30(9):1312–1313. https://doi.org/10.1093/bioinformatics/btu033

Stamatakis A, Hoover P, Rougemont J (2008) A fast bootstrapping algorithm for the RAxML web-servers. Syst Biol 57:758–771. https://doi.org/10.1080/10635150802429642

Swofford DL (2002) PAUP*. Phylogenetic analysis using parsimony (*and other methods). Version 4. Sinauer Associates, Sunderland, Massachusetts

Thiers B (2013) Index Herbariorum: a global directory of public herbaria and associated staff. New York Botanical Garde's Virtual Herbarium. http://sweetgum.nybg.org/ih

Van Vooren N, Moreau P-A (2009) Essai taxinomique sur le genre *Gyromitra* Fr. *sensu lato* (*Pezizales*). 3. Le genre *Gyromitra* Fr., sous-genre *Discina*. Ascomycete.org 1(2):3–13. https://doi.org/10.25664/art-0003

Vassiljeva LN (1950) Species novae fungorum. Notulae Systematicae e Sectione Cryptogamica Instituti Botanici Nomine V.L. Komarovii Academiae Scientificae USSR. 6:188–200

Wang X-C, Zhuang W-Y (2019) A three-locus phylogeny of *Gyromitra* (*Discinaceae*, *Pezizales*) and discovery of two cryptic species. Mycologia 111(1):69–77. https://doi.org/10.1080/00275514.2018.1515456